Accuracy Modelling and Analysis for a Lock-or-Release Mechanism of the Chinese Space Station Microgravity Platform

Jian Ding [a], Jinguo Liu [a,*], Rongpeng Zhang [a], Lu Zhang [b], Guangbo Hao [c]
[a] State Key Laboratory of Robotics, Shenyang Institute of Automation, Chinese Academy of Science, Shenyang, China
[b] Key Laboratory of Space Utilization, Technology and Engineering Center for space Utilization, Chinese Academy of Sciences, Beijing, China.
[c] School of Engineering-Electrical and Electronic Engineering, University College Cork, Cork, Ireland
Corresponding author: Jinguo Liu, State Key Laboratory of Robotics, Shenyang Institute of Automation, Chinese Academy of Sciences, Shenyang, China
Email: liujinguo@sia.cn

ABSTRACT
With development of Chinese space science and technology, plenty of microgravity experiments will be conducted in the Chinese Space Station to be built, and therefore demand for high-precision electromechanical equipment increases substantially. In this paper, a comprehensive accuracy analysis of a new type of auto lock-or-release (L/R) mechanism, which is applied in the Space Station Microgravity Platform (SSMP), is implemented. Firstly, two models (vector analysis model and vector differential model) are, therefore, proposed to analyze output errors of the mechanism. Due to transmission errors from the transmission chain of the gear mechanism, influence factors on axial errors of lead screws are analyzed using design of experiment (DOE) for factor sensitivities. It shows that manufacturing tolerances of the lead screw is the dominant factor. Then, verification of the two proposed accuracy models is comparatively implemented through Monte Carlo (MC) simulation and DOE. Using the present accuracy model, location errors of the lead screw throughout the mechanism's working stroke are illustrated, where the non-synchronous error of the mechanism is particularly discussed. A linear relation between the variance of the non-synchronous error and that of the structural error is established, followed by analyzing influence factors on the non-synchronous error.
Keywords: L/R mechanism, geometrical error, transmission error, Monte Carlo simulation, non-synchronous error

1. Introduction

Around 2020, China is going to complete and operate the near-earth Chinese Space Station, which will become an important base for space science research and new technology experiments such as materials sciences, microgravity fluid physics and biotechnology [1-5]. The conceptual model of the Chinese Space Station, as shown in Fig. 1, is composed of a core chamber module and four experimental chamber modules. In each experimental module, scientific research experimental racks are fixed in parallel. Two auto L/R mechanisms are assembled into both sides of each scientific research experimental rack. The SSMP, which provides a higher level of controllable environment suitable for delicate manipulation for diverse experiments, is locked by

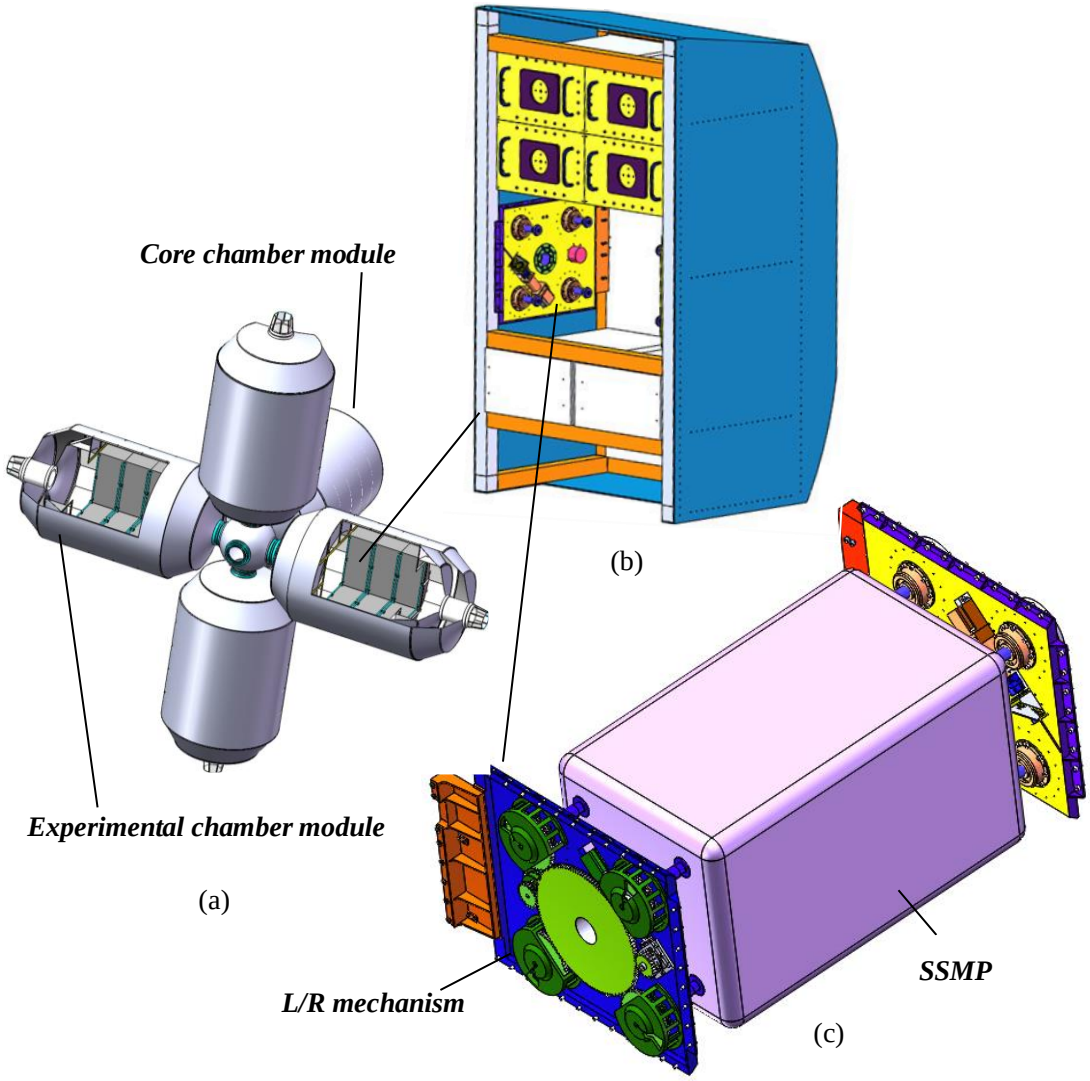

Fig. 1. Hierarchical relation, (a) conceptual model of China Space Station; (b) scientific research experimental rack; (c) two L/R mechanisms with SSMP in a locked status.

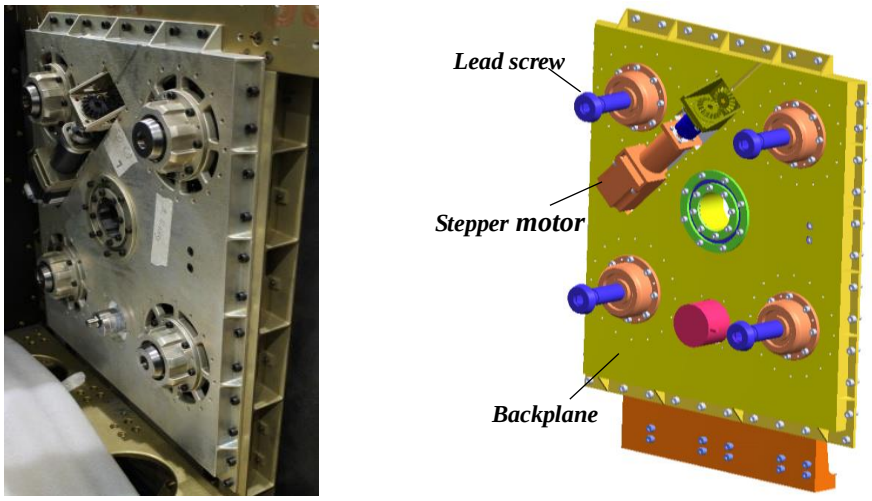

Fig. 2. Architecture of a L/R mechanism on a side of SSMP, (a) physical model; (b) 3D model.

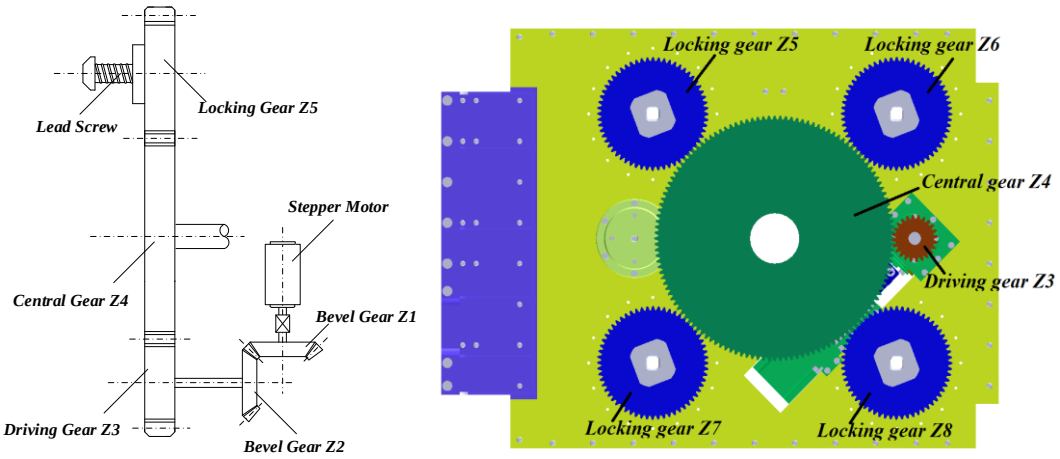

(a) (b)

Fig. 3. Configuration of transmission train of L/R mechanism, (a) scheme of the transmission train; (b) layout of engaged gears on the backplane.

the two L/R mechanisms. As a type of complicated mechatronic equipment, the auto L/R mechanism system responds to high demands on kinematic accuracy, reliability and stability. This research intends to investigate this mechanism in terms of accuracy modelling and analysis, which can find out sensitive factors influencing the output accuracy to promote accuracy performance.

The L/R mechanism is analogous to the parallel-type mechanisms in its structure [6-9]. Huang [10] proposed a comprehensive methodology for insuring geometrical pose accuracy of a 4-DOF (degrees of freedom) pick-and-place robot. In this work, all possible source errors are considered in the error model, and those structural errors, which cannot be compensated for, are restrained via sensitivity analysis. A linear and real-time compensator has been developed and implemented so that critical output accuracy over workspace is achieved by an experimental verification. Jawale [11] made a comprehensive investigation on the open-chain and closed-chain manipulators with two-DOF, focusing on positional accuracy related to joint clearance. An error index using a dimensionless number is defined to evaluate output behavior comparatively. Gojtan [12] presented a simple and light asymmetric parallel mechanism for milling machining applications, the mapping of tool positional errors throughout the available workspace are discussed in detail. Fu [13] investigated the kinematics accuracy problem of a novel 6-dof parallel robot TLPM. The effects of location of the U-joint errors, clearance and driving errors are addressed, the pose errors in some region within workspace reach to high values, and results shows magnitudes of output errors performs nonlinear cumulative trends. The calibration procedure for U-joint errors, clearance, and active joint errors finally confirms the effectiveness of the error model. Li [14] established an angular error model for a multi-loop structure induced by clearances of single joint, multi-joint and locked joint, and explicit solutions for angular errors are obtained. The studied errors conform to Gaussian distribution that is indicated through the analysis of probability density function and finally verified with Monte Carlo simulation. Cui [15] established the position and orientation error model for a 3-DOF 3-PUU parallel robot manipulator, and error sensitivity indexes are employed and evaluated the kinematic accuracy. Then reliability model for kinematic accuracy is formed considering both the controllable and uncontrollable impact. Finally, the mechanism's reliability is analyzed with Monte Carlo simulation.

The accuracy research on parallel-type robots mainly concerns accuracy analysis and synthesis,

as well as geometrical calibration. Accuracy analysis [16-24] is a process of evaluation or verification on output accuracy performance with geometrical errors based on established accuracy model. Accuracy synthesis [25-31], as generally agreed to be an optimum allocation for component tolerances under the condition of various assembly indices, aims at achieving specified optimization such as reducing cost. Geometrical calibration [32-34] is an identification process for parameters of kinematic model by advanced measuring instruments, based on certain identification models.

The rest of this article is organized as follows. Section 2 briefly introduce the working principle of the L/R mechanism. In Section 3, both vector analysis and vector differential models are proposed. In Section 4, the transmission system (gear train) of the L/R mechanism is investigated and significant factors affecting lead screw movement accuracy are comprehensively analyzed. A DOE based method is employed to verify both accuracy models in a comparative way in Section 5, followed by evaluating the error of a lead screw. The non-synchronous errors of the L/R mechanism are also studied statistically with discussions on significant factors. Section 6 finally draws the conclusions.

2. Elaboration of the L/R mechanism

The architecture of a L/R mechanism is illustrated in Fig. 2. The stepper motor, on the backside of the L/R mechanism, drives the bevel gear Z1, then revolves gears Z2 and Z3 that are connected together presented in Fig. 3(a). Driven by a central gear Z4, four branches of gears rotate simultaneously, making four lead screws move forward as synchronous as possible for finally locking gears Z5, Z6, Z7, and Z8, as illustrated in Fig. 3(b). The SSMP is securely locked by contacting the ends of the four lead screws in each L/R mechanism with the slots on each side surface of the SSMP. While arriving at a scheduled orbit of the space station, the four lead screws on each side are then driven to travel inversely to release the SSMP. There may be two problems with the locking. On the one hand, the contact backlash, between ends of the lead screws and the slots of each side of the SSMP, which is mainly induced by location errors and non-synchronous errors of lead screws of the L/R mechanism, tends to result in impact damage of components due to harmonic response from vibration during the launch phase. On the other hand, the SSMP could not form a desired contact status due to the errors of the ends of the lead screws, so the preloading to SSMP by the lead screws could not lead to a symmetric and regular deformation. In such a situation, the SSMP is unstable in locking and can be very dangerous during a dynamic response. Therefore, a comprehensive accuracy modelling and analysis of the L/R mechanism are critical for vouching the system's high reliability and security.

Output accuracy of a mechanism is closely related to its source errors due to geometrical uncertainty. In each L/R mechanism, the output errors refer to the location errors of the end of each lead screw, and the non-synchronous error represents the maximal axial difference of the ends of four lead screws perpendicular to the locking side surface of the SSMP. To ensure that the SSMP is precisely locked or fixed and that associated optical and measuring instruments can work with a high precision throughout the whole process, the output accuracy and non-synchronous accuracy of the L/R mechanism should be improved in the manufacturing stage. As the reflection of critical technical criteria, factors affecting the end error of each lead screw and the non-synchronous error among these lead screws should be investigated.

3. Accuracy modeling

Geometrical errors of the L/R mechanism come from uncertainty of components connected during manufacturing and assembly stages and complicate the influence factors of output errors represented by the end errors of lead screws along three axes. Two approaches of accuracy modeling are presented in this section. A vector analysis model (VAM) could provide an intuitive view for each structural error but could not reveal inner relations between geometrical errors and output errors. A vector differential model (VDM) takes advantage of vector differential algorithms, and provides linear relations between geometrical errors and output errors.

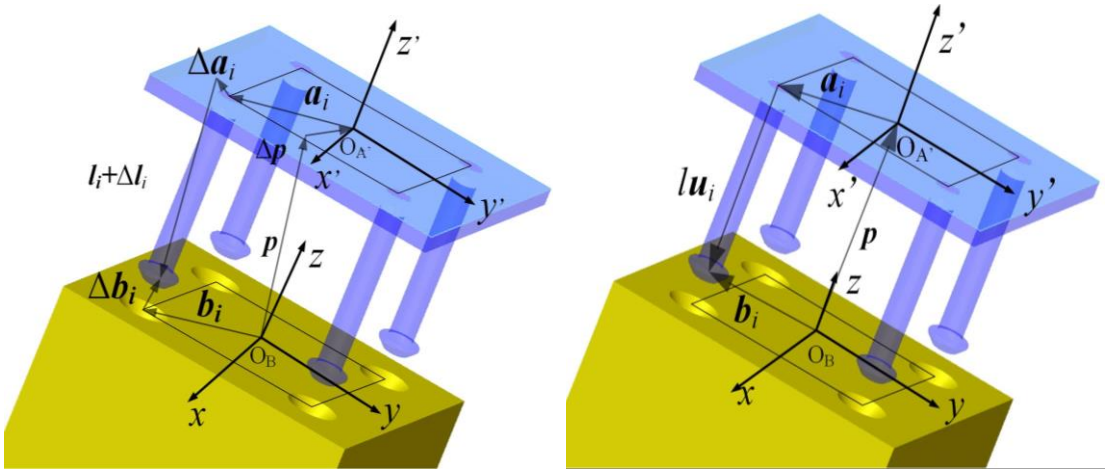

(a) (b)

Fig. 4. Kinematic diagrams for (a) VAM; (b) VDM.

2.1. Vector analysis model (VAM)

The L/R mechanism on one side of the SSMP is depicted in Fig. 4. Since both L/R mechanisms are symmetric with regard to the SSMP, either can provide enough information for accuracy analysis in this paper. Four lead screws are fixed on the backplane of the L/R mechanism, and they are driven by a gear train to synchronously travel forward until their ends contact with slots on the surface of the SSMP. The micro deflection of the SSMP surface, due to locking forces acting on the contact area, can be omitted since the deflection effect is trivial compared to the geometrical errors.

To formulate relations between geometrical and output errors, the end errors of a lead screw, frames, center points and related vectors are defined in Fig. 4(a). $\{O_B\}$ and $\{O_{A'}\}$ are two coordinate frames attached at the two centers on one surface of the SSMP and the backplane of the L/R mechanism, respectively. Frame $\{O_{A'}\}$ has an angular error vector $(\Delta\alpha, \Delta\beta, \Delta\gamma)^T$ and a displacement error vector $(\Delta x, \Delta y, \Delta z)^T$ with respect to the frame$\{O_B\}$ as the base frame. Four lead screws in both coordinate frames form four closed kinematic loops. Since all the lead screws are centrosymmetric about the z'-axis of coordinate frame $\{O_{A'}\}$, either closed kinematic loop is representative and its associate equation can be established as follows

$$\Delta\boldsymbol{b}_i = (\boldsymbol{p}+\Delta\boldsymbol{p}) + \mathbf{R}_1(\boldsymbol{a}_i+\Delta\boldsymbol{a}_i) + \mathbf{R}_2(\boldsymbol{l}_i+\Delta\boldsymbol{l}_i) - \boldsymbol{b}_i \quad (i=1, 2, 3 \text{ or } 4) \tag{1}$$

where $\Delta\boldsymbol{b}_i$ denotes the end error vector of the ith lead screw shown in Fig. 4(a); $\boldsymbol{p}$ and $\Delta\boldsymbol{p}$ are the nominal displacement and its error of frame $\{O_{A'}\}$ with respect to base frame $\{O_B\}$, respectively; $\mathbf{R}_1$ refers to the rotational matrix of frame $\{O_{A'}\}$ with respect to base frame $\{O_B\}$, with orientation

errors, $\Delta\alpha$, $\Delta\beta$, and $\Delta\gamma$, about *x*-, *y*- and *z*- axes of base frame $\{O_B\}$, respectively.
In Eq. (1), $\mathbf{R}_1$ can be expressed as

$$\mathbf{R}_1 = \begin{bmatrix} 1 & -\Delta\gamma & 0 \\ \Delta\gamma & 1 & 0 \\ 0 & 0 & 1 \end{bmatrix} \begin{bmatrix} 1 & 0 & \Delta\beta \\ 0 & 1 & 0 \\ -\Delta\beta & 0 & 1 \end{bmatrix} \begin{bmatrix} 1 & 0 & 0 \\ 0 & 1 & -\Delta\alpha \\ 0 & \Delta\alpha & 1 \end{bmatrix}$$

where $\boldsymbol{a}_i$ and $\Delta\boldsymbol{a}_i$ refer to the nominal position and its error of the *i*th lead screw in the frame $\{O_{A'}\}$. Since there is a micro rotation for frame $\{O_{A'}\}$ with regard to frame $\{O_B\}$, both vectors can be measured in base frame $\{O_B\}$.

In Eq. (1), $\mathbf{R}_2$ is a hybrid rotational matrix for the *i*th lead screw. It first reflects the micro rotations with $\Delta\theta_1$ and $\Delta\theta_2$ with respect to *x*-, *y*-axes in frame $\{O_{A'}\}$, respectively, which reveal the vertical error due to manufacture and assembly uncertainty. It then reflects the rotation of the lead screw and frame $\{O_{A'}\}$ together with respect to base frame $\{O_B\}$. Their consecutive rotational matrix can be described as

$$\mathbf{R}_2 = \mathbf{R}_1 \begin{bmatrix} 1 & 0 & \Delta\theta_2 \\ 0 & 1 & 0 \\ -\Delta\theta_2 & 0 & 1 \end{bmatrix} \begin{bmatrix} 1 & 0 & 0 \\ 0 & 1 & -\Delta\theta_1 \\ 0 & \Delta\theta_1 & 1 \end{bmatrix}$$

where $\boldsymbol{l}_i$ and $\Delta\boldsymbol{l}_i$ denote the nominal axial vector and its error of the *i*th lead screw, which are defined in frame $\{O_{A'}\}$; $\boldsymbol{b}_i$ denotes the nominal vector of an ideal contact between the *i*th slot on SSMP and the end of the *i*th lead screw in base frame $\{O_B\}$. Therefore, by neglecting the higher-order terms associated with the structural error , Eq.(1) can be expressed as follows

$$\begin{cases} \Delta b_{ix} = \Delta x_p + \Delta\beta(a_{iz} - l_i) - \Delta\gamma a_{iy} + \Delta a_{ix} - \Delta\theta_2 l_i - \Delta\gamma\Delta\theta_1 l_i \\ \Delta b_{iy} = \Delta y_p + \Delta\gamma a_{ix} + \Delta\alpha(l_i - a_{iz}) + \Delta a_{iy} + \Delta\theta_1 l_i - \Delta\gamma\Delta\theta_2 l_i \\ \Delta b_{iz} = \Delta z_p + \Delta\alpha a_{iy} - \Delta\beta a_{ix} + \Delta a_{iz} - \Delta l_i + \Delta\alpha\Delta\theta_1 l_i + \Delta\beta\Delta\theta_2 l_i \end{cases} \quad (2)$$

The above-established model for output errors contains sufficient possible structural errors, however, it is difficult to reveal appropriate relations between output and structural errors. Using Monte Carlo simulations can well analyze statistics characteristics of output errors in this model. Note that the VDM that can reveal a linear relationship among errors is developed in the following section.

2.2. Vector differential model (VDM)

In Fig. 4(b), a closed-loop kinematic chain O_B-$O_{A'}$-A_i'-B_i' is formed, a vector equation can be formulated as

$$\boldsymbol{b}_i = \boldsymbol{p} + \mathbf{R}(\boldsymbol{a}_i + l\boldsymbol{u}_i) \quad (i = 1, 2, 3 \text{ or } 4) \quad (3)$$

where $\mathbf{R}$ denotes the rotational matrix of frame $\{O_{A'}\}$ with respect to base frame $\{O_B\}$, with orientation nominal parameters, α, β, and γ, about *x*-, *y*- and *z*- axes of base frame $\{O_B\}$, respectively**,** which can be expressed as

$$\mathbf{R}=\begin{bmatrix}\cos\gamma & -\sin\gamma & 0\\ \sin\gamma & \cos\gamma & 0\\ 0 & 0 & 1\end{bmatrix}\begin{bmatrix}\cos\beta & 0 & \sin\beta\\ 0 & 1 & 0\\ -\sin\beta & 0 & \cos\beta\end{bmatrix}\begin{bmatrix}1 & 0 & 0\\ 0 & \cos\alpha & -\sin\alpha\\ 0 & \sin\alpha & \cos\alpha\end{bmatrix}$$

Differentiating both sides of Eq. (3) yields

$$\delta\boldsymbol{b}_i=\delta\boldsymbol{p}+\delta\mathbf{R}\left(\boldsymbol{a}_i+l_i\cdot\boldsymbol{u}_i\right)+\mathbf{R}\left(\delta\boldsymbol{a}_i+\delta l\cdot\boldsymbol{u}_i+l\cdot\delta\boldsymbol{u}_i\right) \tag{4}$$

where $\delta\boldsymbol{b}_i$ refers to the end errors of the ith lead screw in frame $\{O_B\}$; $\delta\boldsymbol{p}$ refers to displacement errors of frame $\{O_{A'}\}$, expressed by $(\delta x_p, \delta y_p, \delta z_p)^T$, with respect to base frame $\{O_B\}$; $\delta\mathbf{R}$ refers to perturbation of the rotational matrix $\mathbf{R}$ of frame $\{O_{A'}\}$ with regard to base frame $\{O_B\}$; $\boldsymbol{u}_i$ denotes an unit vector of the ith lead screw, and is detailed by $(u_x, u_y, u_z)^T$; $\delta\boldsymbol{u}_i$ represents a deviation of $\boldsymbol{u}_i$, expressed as

$$\delta\boldsymbol{u}_i=\Delta_{\boldsymbol{u}_i}\boldsymbol{u}_i=\begin{bmatrix}0 & -\delta u_z & \delta u_y\\ \delta u_z & 0 & -\delta u_x\\ -\delta u_y & \delta u_x & 0\end{bmatrix}\begin{bmatrix}u_x\\ u_y\\ u_z\end{bmatrix}$$

where Δ_{ui} is an antisymmetric tensor of $\delta\boldsymbol{u}_i$.

For $\delta\mathbf{R}$ in Eq. (4), the perturbation vector $\delta\boldsymbol{\Omega}$ $(\delta\Omega_x, \delta\Omega_y, \delta\Omega_z)^T$ of the nominal angles α, β, and γ, with respect to base frame $\{O_B\}$, can be expressed as

$$\delta\Omega=\delta\gamma\begin{bmatrix}0\\ 0\\ 1\end{bmatrix}+\delta\beta\begin{bmatrix}\cos\gamma & -\sin\gamma & 0\\ \sin\gamma & \cos\gamma & 0\\ 0 & 0 & 1\end{bmatrix}\begin{bmatrix}0\\ 1\\ 0\end{bmatrix}+\delta\alpha\begin{bmatrix}\cos\gamma & -\sin\gamma & 0\\ \sin\gamma & \cos\gamma & 0\\ 0 & 0 & 1\end{bmatrix}\begin{bmatrix}\cos\beta & 0 & \sin\beta\\ 0 & 1 & 0\\ -\sin\beta & 0 & \cos\beta\end{bmatrix}\begin{bmatrix}1\\ 0\\ 0\end{bmatrix}$$

$$\delta\Omega=\begin{bmatrix}\delta\Omega_x\\ \delta\Omega_y\\ \delta\Omega_z\end{bmatrix}=\begin{bmatrix}-\sin\gamma\delta\beta+\cos\gamma\cos\beta\delta\alpha\\ \cos\gamma\delta\beta+\sin\gamma\cos\beta\delta\alpha\\ -\sin\beta\delta\alpha+\delta\gamma\end{bmatrix}$$

The antisymmetric tensor of $\delta\boldsymbol{\Omega}$ can be denoted as

$$\Delta_R=\begin{bmatrix}0 & -\delta\Omega_z & \delta\Omega_y\\ \delta\Omega_z & 0 & -\delta\Omega_x\\ -\delta\Omega_y & \delta\Omega_x & 0\end{bmatrix}$$

Therefore, the matrix $\delta\mathbf{R}$ in Eq.(4) can be written as

$$\delta\mathbf{R}=\Delta_R\mathbf{R}=\begin{bmatrix}0 & \sin\beta\delta\alpha-\delta\gamma & \cos\gamma\delta\beta+\sin\gamma\cos\beta\delta\alpha\\ -\sin\beta\delta\alpha+\delta\gamma & 0 & \sin\gamma\delta\beta-\cos\gamma\cos\beta\delta\alpha\\ -\cos\gamma\delta\beta-\sin\gamma\cos\beta\delta\alpha & -\sin\gamma\delta\beta+\cos\gamma\cos\beta\delta\alpha & 0\end{bmatrix}\mathbf{R}$$

Since the nominal orientation angles α, β, and γ, of the frame $\{O_{A'}\}$ with respect to base frame $\{O_B\}$ are all zeros in the geometric configuration of the SSMP and the L/R mechanism, $\delta\mathbf{R}$ can be simplified as

$$\delta\mathbf{R}=\Delta_R\mathbf{R}=\begin{bmatrix}0 & -\delta\gamma & \delta\beta\\ \delta\gamma & 0 & -\delta\alpha\\ -\delta\beta & \delta\alpha & 0\end{bmatrix}\mathbf{R}$$

Let $\boldsymbol{c}_i$=$\mathbf{R}$($\boldsymbol{a}_i$+$l_i\boldsymbol{u}_i$), Eq. (4) can be rewritten in a compact form as below:

$$\delta \boldsymbol{b}_i = \begin{bmatrix} \mathbf{E} & \Delta_{\boldsymbol{c}_i}^T \end{bmatrix} \begin{bmatrix} \delta \boldsymbol{p} \\ \delta \boldsymbol{\Omega} \end{bmatrix} + \mathbf{R} \cdot \left(\delta \boldsymbol{a}_i + \delta l \cdot \boldsymbol{u}_i + l \cdot \Delta_{\boldsymbol{u}_i} \cdot \boldsymbol{u}_i \right) \tag{5}$$

where $\mathbf{E}$ is a 3×3 unit matrix; $\Delta_{\boldsymbol{c}i}$ is an antisymmetric tensor of vector $\boldsymbol{c}_i$.

According to assembly requirements for the backplane of the L/R mechanism, nominal parameters in Eq. (5) are determined in advance. The nominal orientation angles α, β, and γ of frame $\{O_{A'}\}$ with respect to base frame $\{O_B\}$ are zeros, so the orientation matrix $\mathbf{R}$ becomes a 3×3 unit matrix. The unit vector $\boldsymbol{u}_i$ ($\boldsymbol{u}_i$ = (0 0 -1)^T) for a lead screw synchronizes with frame $\{O_{A'}\}$ while micro rotating of frame $\{O_{A'}\}$ occurs. Both micro rotational errors, $\Delta\theta_1$ and $\Delta\theta_2$, for a lead screw about its own x- and y-axes, under the constraint of perpendicularity to backplane, so z-component of $\boldsymbol{u}_i$ is zero. The x- and y-components of $\delta\boldsymbol{u}_i$ can be approximated with micro rotational angles, $\Delta\theta_1$ and $\Delta\theta_2$, respectively.

Thus, Eq. (5) can be unfolded as follows

$$\begin{bmatrix} \delta b_{ix} \\ \delta b_{iy} \\ \delta b_{iz} \end{bmatrix} = \begin{bmatrix} 1 & 0 & 0 & 0 & a_{iz}-l_i & -a_{iy} \\ 0 & 1 & 0 & l_i-a_{iz} & 0 & a_{ix} \\ 0 & 0 & 1 & a_{iy} & -a_{ix} & 0 \end{bmatrix} \begin{bmatrix} \delta x_p \\ \delta y_p \\ \delta z_p \\ \delta\alpha \\ \delta\beta \\ \delta\gamma \end{bmatrix} + \begin{bmatrix} \delta a_{ix} \\ \delta a_{iy} \\ \delta a_{iz} \end{bmatrix} + \begin{bmatrix} 0 \\ 0 \\ -\delta l_i \end{bmatrix} + l \begin{bmatrix} 0 & -\delta u_{iz} & \delta u_{iy} \\ \delta u_{iz} & 0 & -\delta u_{ix} \\ -\delta u_{iy} & \delta u_{ix} & 0 \end{bmatrix} \begin{bmatrix} 0 \\ 0 \\ -1 \end{bmatrix} \tag{6}$$

As one of dominant geometrical errors, the axial error Δl of each lead screw is contributed by the gear train in the L/R mechanism, and is irrelevant with other geometrical errors investigated above. Therefore, there is a necessity to give a comprehensive analysis on the transmission system, in order to find out significant factors contributing to axial error Δl of each lead screw.

4. Transmission accuracy analysis

As is shown in Fig. 3, a perfect synchronous process without any axial differences for four lead screws of each L/R mechanism could not be achieved, since stochastic backlashes in the sub-chain from the central gear Z4 to the lead screw result in difference of output axial errors of lead screws. The transmission error from engaged gears to lead screws in the gear train plays a significant influence on axial errors of lead screws. Major attention should be given to the backlash due to gears' engagement for studying axial error Δl of a lead screw. Therefore, it is necessary to investigate factors induced by manufacturing and assembly process.

2.3. Transmission errors analysis

It is widely accepted that transmission errors of a gear train system mainly result from manufacturing and assembly uncertainty. Generally speaking, manufacturing errors of a cylindrical gear for instance are induced from the coupling effects of geometric eccentric, kinematic eccentric, profile deviation and tooth thickness deviation and so on. The assembly error of a gear is formed by deviations of its actual rotation center with respect to its ideal rotational center, with remarkable factors including gear central distance offset, fit clearance between gear and rotary shaft, and radical clearance of a bearing [35].

Detailed influences on transmission errors include a gear single transmission error K, a circumferential backlash j, and an axial error of a lead screw Δl_s.

For the gear single transmission error K, it is primarily from the gear tangential total composite

deviation F_i', which includes the total cumulative pitch deviation F_p and the single tooth tangential composite deviation f_i', can be denoted as

$$K_i \approx F_i' = F_p + f_i' \tag{7}$$

For the circumferential backlash j, it is induced by a tooth thickness deviation, a gear central distance offset, and a bearing radical clearance, etc.

The manufacturing error for a single gear contributes to the backlash of gear engagement in assembled process. The circumferential backlash induced by pith deviation of engaged gears is written as

$$j_1 = E_{s1} + E_{s2} \tag{8}$$

where E_{s1} and E_{s2} denote tolerance of tooth thickness of engaged gears 1 and 2, respectively.

The circumferential backlash induced by the gear central distance offset can be expressed as

$$j_2 = 2 f_a \tan \alpha_v \tag{9}$$

where f_a denotes a central distance offset of engaged gears; α_v denotes a normal pressure angle of engaged teeth.

The circumferential backlash induced by the radical clearance of bearing can be expressed as

$$j_3 = 2(u_1 + u_2) \tan \alpha_v \tag{10}$$

where u_1 and u_2 refer to radical clearance of bearings matching with gears 1 and 2, respectively.

As the end of the transmission chain, the axial error of a lead screw includes two aspects: the manufacturing precision level of a lead screw denoted as Δl_s; and the circular pitch error accumulated in the locking gear Z5/ Z6/ Z7/ Z8 from the forward transmission chain. Thus, the total axial error of a lead screw can be written as

$$\Delta l = \Delta l_s + \frac{s}{\pi d}(K_1 + K_2 + \sum_{i=1}^{3} j_i) \tag{11}$$

where Δl refers to the total output axial error of a lead screw and is used in Eq. (6); Δl_s refers to the manufacturing error of a lead screw; d denotes to the diameter of pitch circle of the locking gear Z5; s denotes to the pitch of a lead screw.

All the components involved in Eq. (11) are independent with each other, the statistic means and standard deviations of the components can be formulated as

$$E(\Delta l) = E(\Delta l_s) + \frac{s}{\pi d} E(K_1 + K_2 + \sum_{i=1}^{3} j_i) \tag{12a}$$

$$\sigma^2(\Delta l) = \sigma^2(\Delta l_s) + \frac{s}{\pi d} \sigma^2(K_1 + K_2 + \sum_{i=1}^{3} j_i) \tag{12b}$$

where E(.) and σ(.) denote the average operator and standard deviation operators in statistics, respectively.

2.4. Sensitivity analysis based on DOE

In the sub-chain from the central gear Z4 to the lead screw discussed above, factors on

influencing output errors of a lead screw are finally determined as follows:

- Factor 1: manufacturing precision of central gear Z4;
- Factor 2: manufacturing precision of locking gear Z5/Z6/Z7/Z8;
- Factor 3: radical clearance of deep groove ball bearing fixed with gear Z4;
- Factor 4: central distance offset of engaged gears of Z4 and Z5/Z6/Z7/Z8;
- Factor 5: axial tolerance of a lead screw (Travel between 40mm-75mm).

The precision grades of engagements are selected based on experience and reference, and are treated as levels of DOE. The standard deviation of the total axial error Δl of a lead screw is selected as a response to DOE. Array $L_{16}(4^5)$ is reasonable to be employed in the DOE as shown in Tables 1 and 2. Using Eq. (12*b*), Each MC simulation with 10^5 samples is conducted for each row in array $L_{16}(4^5)$. Detailed arrangement and application for DOE are tabulated in Tables 1 and 2.

Table 1

Levels arrangements for DOE with array $L_{16}(4^5)$ (central distance offset of engaged gears with quasi-level).

level	Factor 1	Factor 2	Factor 3	Factor 4	Factor 5
1	Grade 4	Grade 4	Grade 2 /15μm	Grade 5~6 /±23μm	Grade 4 /2.67μm
2	Grade 5	Grade 5	Grade 0 /30μm	Grade 7~8 /±36μm	Grade 5 /4.17μm
3	Grade 6	Grade 6	Grade 3 /51μm	Grade 9~10 /±57.5μm	Grade 6 /7.67μm
4	Grade 7	Grade 7	Grade 4 /71μm	Grade 7~8 /±36μm (quasi-level)	Grade 7 /10.56μm

Table 2

Quasi-level DOE with array $L_{16}(4^5)$.

	Factor 1	Factor 2	Factor 3	Factor 4	Factor 5	Response /μm
1	Grade4	Grade4	Grade 2/15	Grade 5~6/±23	Grade 4/2.67	0.646
2	Grade4	Grade5	Grade 0/30	Grade 7~8/±36	Grade 5/4.17	0.844
3	Grade4	Grade6	Grade 3/51	Grade 9~10/±57.5	Grade 6/7.67	1.371
4	Grade4	Grade7	Grade 4/71	Grade7~8/±36	Grade 7/10.56	1.835
5	Grade5	Grade4	Grade 0/30	Grade 9~10 /±57.5	Grade 7 /10.56	1.827
6	Grade5	Grade5	Grade 2/15	Grade7~8/±36	Grade 6 /7.67	1.371
7	Grade5	Grade6	Grade 4/71	Grade 5~6 /±23	Grade 5 /4.17	0.863
8	Grade5	Grade7	Grade 3/51	Grade 7~8/±36	Grade 4 /2.67	0.695
9	Grade6	Grade4	Grade 3/51	Grade7~8/±36	Grade 5 /4.17	0.862
10	Grade6	Grade5	Grade 4/71	Grade 9~10 /±57.5	Grade 4 /2.67	0.687
11	Grade6	Grade6	Grade 2/15	Grade 7~8/±36	Grade 7 /10.56	1.840
12	Grade6	Grade7	Grade 0/30	Grade 5~6 /±23	Grade 6 /7.67	1.394
13	Grade7	Grade4	Grade 4/71	Grade 7~8/±36	Grade 6 /7.67	1.389
14	Grade7	Grade5	Grade 3/51	Grade 5~6 /±23	Grade 7 /10.56	1.845
15	Grade7	Grade6	Grade 0/30	Grade7~8/±36	Grade 4 /2.67	0.722
16	Grade7	Grade7	Grade 2/15	Grade 9~10 /±57.5	Grade 5 /4.17	0.912

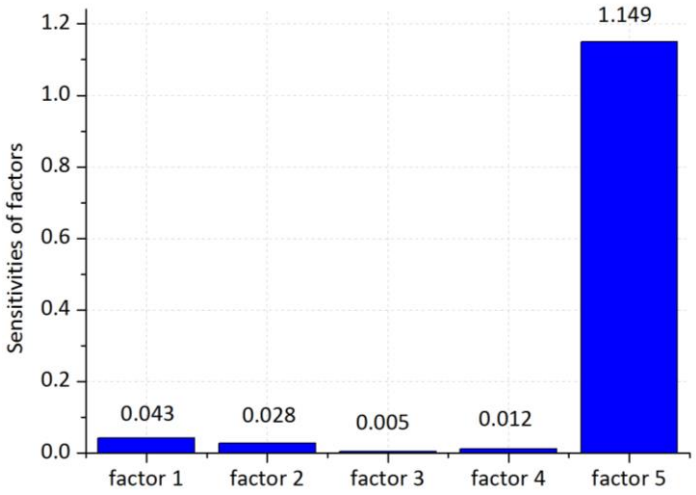

Fig. 5. Sensitivity analysis for factors influencing axial error Δl of a lead screw

Table 3

Analysis of variance with factor sensitivities for significance.

Source of variation	Sum of squares	Degrees of freedom	Mean square	F_0
Factor 5	3.237	3	1.079	41641.5*
Factor 1	3.860×10^{-3}	3	1.287×10^{-3}	49.657
Factor 2	1.872×10^{-3}	3	6.241×10^{-4}	24.086
Factor 4	3.079×10^{-4}	2	1.539×10^{-4}	5.941
SS_e^{Δ} including Factor 3	1.037×10^{-4}	4	2.591×10^{-5}	——
SS_t	3.243	15	——	——

Significance at $F_{0.005}(3,1)$ =21615

Analysis is conducted with DOE array $L_{16}(4^5)$ for sensitivities of factors in the transmission chain, with results shown in Fig. 5 and Table 3. It is demonstrated that the two types of analysis produce the similar result. Consensus indicates that among these investigated factors in the transmission chain, the precision of a manufactured lead screw (reflected by Δl_s) is the most significant one for affecting the axial output error Δl of a lead screw. The precision level of a manufactured lead screw should be primarily improved as a higher accuracy for this transmission chain is required. As for the other influencing factors, their tolerances can be enlarged properly which would hardly harm output accuracy of the transmission chain.

5. Accuracy verification and analysis

3.1. Comparative verifications

The VAM for the L/R mechanism's output errors could directly obtain reliable output errors (the end errors of lead screws) since this modelling methodology has been applied widely, however it could not reflect the linear relationship between output and geometrical errors. The presented VDM can avoid this problem by employing a first order approximation to output errors of the L/R mechanism, which omits geometrical errors with 2nd and higher order infinitesimals. In practical

application for the L/R mechanism's accuracy analysis, there is a necessity to make a comparison for output errors from both models before being putting into application, whether the VDM is precise enough to satisfy accuracy analysis for the L/R mechanism.

The VDM that uses Monte Carlo simulations, in terms of nominal geometrical parameters and related structural errors, is applied for statistics analysis of output errors, in comparison to the VAM for the verification process. The output accuracy analysis employs a set of 10 types of structural errors in terms of Eq. (6). The statistics theories have suggested [36] that the ultimate lead screw's end errors always conform to a Gaussian distribution as long as there are more than 6 types of errors, regardless of the distribution of each type of error.

A DOE array is utilized to ensure a comprehensive and rigorous verification. The arrangements of a DOE array mathematically represent different test points distributed uniformly and ergodically in the experimental space. If the difference of output errors' statistics of the L/R mechanism obtained from two accuracy models are kept in an acceptable range, the two models can be mutually verified. Since the VAM is intuitive to enable its correctness being guaranteed easily, therefore, it is used to verify the VDM. Structural errors are treated as different influence factors, and the scopes of which are then divided into different levels correspondingly. Monte Carlo simulations with each arrangement using both accuracy models established above are implemented to yield output errors' statistics.

Structural parameters of the L/R mechanism with regard to the SSMP side surface include its backplane displacement along *z*- axis (60mm), and those along *x*-, *y*- axes (both zeros). Table 4 indicates the nominal parameters of the starting ends and contact (distal) ends of lead screws. The movement stroke of lead screws is set to 60mm. All the geometrical errors are assumed to conform to Gaussian distribution with their mean of zeros. Considering that a feasible DOE array should include at least 10 factors, for a more uniform and adaptive comparison, the $U_{25}(5^{10})$ array is selected where divisions for structural errors are subsequently tabulated in Table 5.

The index e_i (i=x, y, z) is used to test the differences of the standard deviation (σ_x, σ_y, or σ_z) of output errors from VAM and VDM, and expressed as

$$e_i = \left| \frac{\sigma_i^{\mathrm{VDM}} - \sigma_i^{\mathrm{VAM}}}{\sigma_i^{\mathrm{VAM}}} \right| \times 100\% \qquad (i=x, y, z) \tag{13}$$

where σ_i^{VDM} represents standard deviation σ_i yielding from VDM; σ_i^{VAM} represents standard deviation σ_i yielding from VAM. If each e_i is within 5% for instance, the VDM is convinced to be precise enough and can be put into application.

Statistics for output errors are processed by Monte Carlo simulations with 10^5 samples for each arrangement in $U_{25}(5^{10})$ array, using VDM. In comparison, the VAM could directly yield means and standard deviations of output errors. For each arrangement in array, once the difference of statistics (obtained from two models) is within permitted computational precision, the VDM approach is acceptable. The result of statistics with both models is simulated and listed in Table 6.

Table 4

Nominal parameters for L/R mechanism.

	Nominal locations of lead screws			Nominal contacts points of lead screws		
	a_x	a_y	a_z	b_x	b_y	b_z
1	150	150	60	150	150	0
2	-150	150	60	-150	150	0

3	-150	-150	60	-150	-150	0
4	150	-150	60	150	-150	0

Table 5

Level divisions of mechanism structural errors for $U_{25}(5^{10})$ array.

	Δx_p /mm	Δy_p /mm	Δz_p /mm	$\Delta a_{ix}/\Delta a_{iy}$ /mm	Δa_{iz} /mm	$\Delta\alpha$ /°	$\Delta\beta$ /°	$\Delta\gamma$ /°	$\Delta\theta_1/\Delta\theta_2$ /°	Δl /mm
Level 1	±0.1	±0.1	±0.1	±0.05	±0.05	±0.1	±0.1	±0.1	±0.06	±0.01
Level 2	±0.15	±0.15	±0.15	±0.1	±0.1	±0.15	±0.15	±0.15	±0.08	±0.02
Level 3	±0.2	±0.2	±0.2	±0.15	±0.15	±0.2	±0.2	±0.2	±0.1	±0.03
Level 4	±0.25	±0.25	±0.25	±0.2	±0.2	±0.25	±0.25	±0.25	±0.12	±0.04
Level 5	±0.3	±0.3	±0.3	±0.25	±0.25	±0.3	±0.3	±0.3	±0.14	±0.05

Table 6

Mean μ and Standard deviations σ for end errors of a lead screw.

	VAM						VDM		
	μ_x ($\times10^{-4}$ mm)	μ_y ($\times10^{-4}$ mm)	μ_z ($\times10^{-4}$ mm)	σ_x (mm)	σ_y (mm)	σ_z (mm)	σ_{x0} (mm)	σ_{y0} (mm)	σ_{z0} (mm)
1	-7.9	6.1	-2.4	0.1527	0.1816	0.2909	0.1519	0.1812	0.2915
2	-2.1	-7	-8.4	0.2293	0.2397	0.2027	0.2296	0.239	0.2021
3	1.3	-8.7	6.3	0.1569	0.1414	0.3312	0.1571	0.1405	0.333
4	7.1	-3.4	15.9	0.2013	0.2224	0.2056	0.2014	0.2225	0.206
5	-2.8	-4.6	1.8	0.278	0.2893	0.2999	0.2787	0.2901	0.2999
6	-0.2	-6.2	2.4	0.2386	0.2282	0.2253	0.2384	0.2279	0.2254
7	-14.1	-1	-22.8	0.1788	0.1846	0.375	0.1795	0.1845	0.3758
8	-3.6	-0.4	-6.3	0.1495	0.1434	0.2069	0.1497	0.1437	0.2068
9	-3.5	7	6.2	0.2408	0.2551	0.2868	0.241	0.255	0.2862
10	-15.9	3.3	-4.4	0.2586	0.2737	0.3472	0.2585	0.2729	0.3455
11	-9.2	5.3	2.9	0.292	0.2915	0.284	0.293	0.2919	0.2828
12	-2.3	-4.7	0.5	0.1471	0.1153	0.2806	0.146	0.1155	0.2811
13	1.6	1.3	-0.1	0.1598	0.1675	0.139	0.1605	0.1679	0.1387
14	2.2	2.8	8.7	0.1704	0.185	0.3029	0.171	0.1856	0.3027
15	-4.8	2.5	-10.2	0.2953	0.2909	0.3054	0.2954	0.2922	0.3059
16	1.6	-3.5	8	0.2273	0.2027	0.2642	0.2268	0.203	0.2633
17	-4.9	-9	-2.3	0.2616	0.2452	0.3523	0.2621	0.246	0.3561
18	-3.4	-6.9	1.5	0.2841	0.2797	0.1496	0.2833	0.2798	0.1497
19	-3.9	-1.5	9.1	0.142	0.168	0.2661	0.1424	0.1681	0.2654
20	1.7	4.8	11.4	0.1813	0.1997	0.2256	0.1813	0.1992	0.2248
21	1.4	-2.5	11.6	0.2115	0.1926	0.1948	0.2103	0.1922	0.1946
22	-2.6	-6.1	-11.6	0.2959	0.2972	0.3014	0.296	0.2984	0.301
23	-6.6	7.5	6.9	0.1775	0.1521	0.2881	0.1775	0.1524	0.2883

24	-0.4	-3.7	-4.9	0.2438	0.216	0.2966	0.2443	0.2166	0.2956
25	5.5	-13.4	-6.8	0.2153	0.2236	0.3311	0.2163	0.2226	0.33

It can be inferred from Table 6 that the mean of output errors for a lead screw using the VAM is no more than 2.28×10^{-3} mm, in contrast with the theoretical mean of zero. This deviation can be accepted since all of input geometrical errors are distributed symmetrically with zero. By comparison with VAM and VDM, the maximal e_x is 0.75%, e_y is 0.64%, and e_z is 1.1%. The differences of the standard deviation (σ_x, σ_y, or σ_z) of output errors, do not exceed a threshold of 5%. It is suggested the presented VDM has enough computational precision to output errors of the L/R mechanism. Therefore, it can be accepted and implemented in accuracy analysis and furthermore in tolerance synthesis for the L/R mechanism, which would yield a reasonable structural tolerance solution.

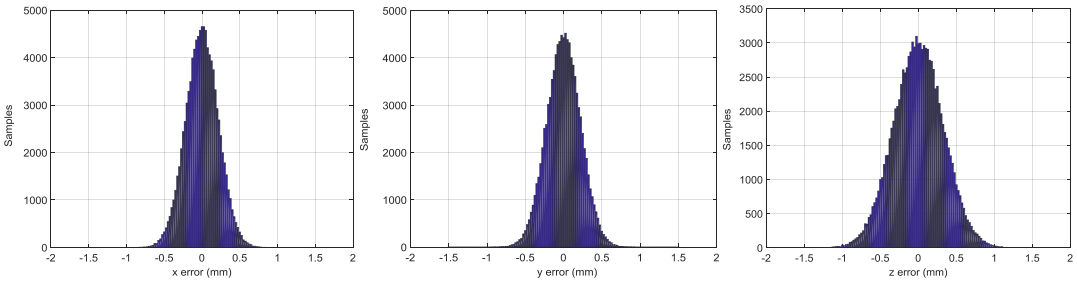

(a) **(b)** **(c)**

Fig. 6. Error distributions for a lead screw, (a) x error; (b) y error; and (c) z error.

Taking the *25*th row in Table 6 above for instance, we can obtain Fig. 6 after a statistic analysis, which describes output errors along *x*-, *y*- and *z*- axes for a lead screw, respectively. Gaussian distributions as expected have been observed and their scopes in terms of the '3σ' principle are ±0.649mm, ±0.668mm, and ±0.99mm, which agree with the results calculated from the VDM.

3.2. Locking position error of a lead screw

Different locking positions for the SSMP yield different errors for a lead screw. In Eq. (6), considering structural parameter a_{iz} of zero and independence among structural errors with each other, a statistic model from Eq. (6) can be represented as follows

$$\sigma^2_{\Delta b_{ix}} = \sigma^2_{\Delta x_p} + l^2\sigma^2_{\Delta\beta} + a^2_{iy}\sigma^2_{\Delta\gamma} + \sigma^2_{\Delta a_{ix}} + l^2\sigma^2_{\Delta u_y} \tag{14a}$$

$$\sigma^2_{\Delta b_{iy}} = \sigma^2_{\Delta y_p} + l^2\sigma^2_{\Delta\alpha} + a^2_{ix}\sigma^2_{\Delta\gamma} + \sigma^2_{\Delta a_{iy}} + l^2\sigma^2_{\Delta u_x} \tag{14b}$$

$$\sigma^2_{\Delta b_{iz}} = \sigma^2_{\Delta z_p} + a^2_{iy}\sigma^2_{\Delta\alpha} + a^2_{ix}\sigma^2_{\Delta\beta} + \sigma^2_{\Delta a_{iz}} + \sigma^2_{\Delta l} \tag{14c}$$

As a lead screw's movement is restricted within 40 mm~75 mm, in terms of structural parameters listed in Table 7, the variations for errors of a lead screw along *x*-, *y*- and *z*- axes can be simulated with Eq. (14) in terms of the '6σ' principle.

Table 7

Geometrical errors for L/R mechanism.

Δx_p	Δy_p	Δz_p	$\Delta a_{ix}/\Delta a_{iy}$	Δa_{iz}	$\Delta\alpha$	$\Delta\beta$	$\Delta\gamma$	$\Delta\theta_1/\Delta\theta_2$	Δl_s

/mm	/mm	/mm	/mm	/mm	/°	/°	/°	/°	/mm
±0.15	±0.2	±0.25	±0.15	±0.25	±0.15	±0.25	±0.3	±0.08	±0.03

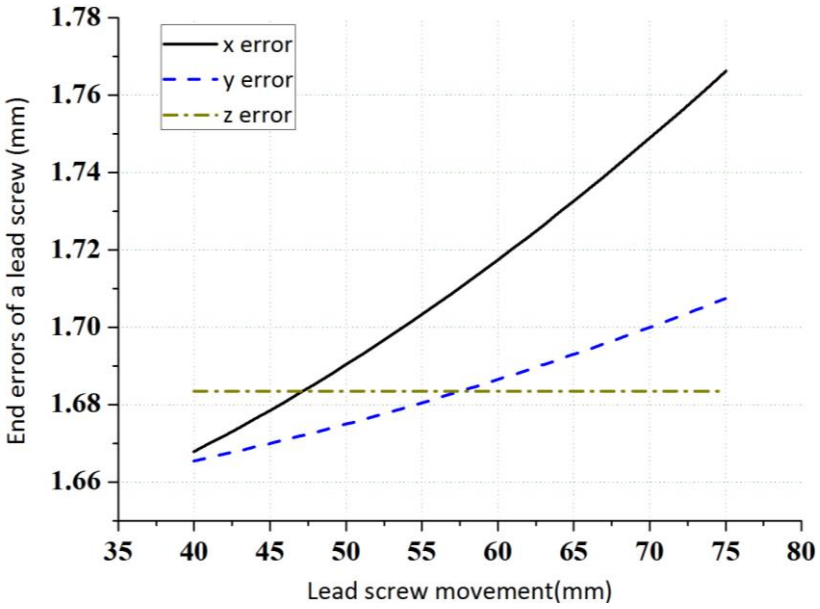

Fig. 7. Variations for output errors of a lead screw along *x*-, *y*- and *z*- axes.

Fig. 7 indicates that as lead screws move the output errors of a lead screw along *x*- and *y*- axes increase and that along *z*- axis keeps constant. It can be seen that the error along the *x*- axis is always larger than that in the *y*- axis. In the initial moving period for a lead screw, the error along *x*-/*y*- axis is less than that along the *z*- axis; as lead screw movement exceeds 58mm, both errors along *x*- and *y*- axes are larger than that along *z*- axis. Within a movement range (40mm~75mm) for a lead screw, the errors along *x*- and *y*- axes between 1.665mm and 1.766mm, and that along *z*- axis keeps constant at 1.683mm.

3.3. Non-synchronous error analysis

The non-synchronous error for lead screws of the L/R mechanism is one of particular errors in accuracy analysis, which represents the maximal difference of the ends of four lead screws along the *z*- axis of coordinate frame $\{O_B\}$ defined in Fig. 4. It differs from a general definition of the position error along *z*- axis as investigated above, which only concerns dimensional error between actual and nominal position at the end of a lead screw with respect to the locking side surface of SSMP. A non-synchronous error among lead screws has a tendency to lead complex contact problems between the SSMP surface and lead screw ends in static or dynamic analysis. The problems can be classified into two folds: a) The uncertain stress-strain state on locked surface of the SSMP and structural deformation compatibility should be investigated due to the non-synchronous error; b) The complex contact stress state inversely causes lead screws to be unevenly pressed so that the bulking stability for lead screws needs to be evaluated. In this sense, research on the non-synchronous error for the L/R mechanism is essential.

Considering this structural symmetry of the mechanism as shown in Table 4, we have

$$|a_{ix}| = |a_{iy}| \quad (i = 1, 2, 3, 4), \tag{15}$$

Let $|a_{ix}|$ and $|a_{iy}|$ be denoted by h, the errors along z axis applied to all lead screws in terms of the accuracy model in Eq. (6) can be simplified as

$$\begin{aligned}
\delta b_{1z} &= \delta z_p + h\delta\alpha - h\delta\beta + \delta a_{1z} - \delta l_1 \\
\delta b_{2z} &= \delta z_p + h\delta\alpha + h\delta\beta + \delta a_{2z} - \delta l_2 \\
\delta b_{3z} &= \delta z_p - h\delta\alpha + h\delta\beta + \delta a_{3z} - \delta l_3 \\
\delta b_{4z} &= \delta z_p - h\delta\alpha - h\delta\beta + \delta a_{4z} - \delta l_4
\end{aligned} \tag{16}$$

Structural errors δa_{iz} (i=1,2,3 or 4) share the same statistics owing to the same manufacturing process, so their standard deviations should be the same. The same conclusion is also applicable to axial error of each lead screw δl_i (i=1,2,3 or 4), meaning that their standard deviations are equal to each other. In Eq. (6), the errors along z- axis for these four lead screws are different with each other, and their difference only lies in the *2*th and *3*th terms for each equation. Once the structural errors are given, the difference between δb_{2z} and δb_{4z} is most significant, so does that between δb_{1z} and δb_{3z}. An observation indicates that the maximal discrepancy along z- axis among four lead screws lies on a pair of lead screws in the diagonal direction rather than a pair of adjacent lead screws. Let δb_{24z} denote an absolute value between δb_{2z} and δb_{4z}, and δb_{13z} denote an absolute value between δb_{1z} and δb_{3z}. It is can be determined that either δb_{24z} or δb_{13z} is more proper to reflect the non-synchronous error for each L/R mechanism. Both of them can be expressed as follows

$$\begin{aligned}
\delta b_{24z} &= 2h\delta\alpha + 2h\delta\beta + \delta a_{2z} - \delta a_{4z} - \delta l_2 + \delta l_4 \\
\delta b_{13z} &= 2h\delta\alpha - 2h\delta\beta + \delta a_{1z} - \delta a_{3z} - \delta l_1 + \delta l_3
\end{aligned} \tag{17}$$

Using statistical analysis, let $\sigma_{\delta b24z}$ denote a standard deviation of δb_{24z}, and $\sigma_{\delta b13z}$ denote a standard deviation of δb_{13z}. Since structural errors are irrelevant with each other, we can obtain

$$\begin{aligned}
\sigma^2_{\delta b24z} &= 4h^2\sigma^2_{\Delta\alpha} + 4h^2\sigma^2_{\Delta\beta} + 2\sigma^2_{\Delta az} + 2\sigma^2_{\Delta l} \\
\sigma^2_{\delta b13z} &= 4h^2\sigma^2_{\Delta\alpha} + 4h^2\sigma^2_{\Delta\beta} + 2\sigma^2_{\Delta az} + 2\sigma^2_{\Delta l}
\end{aligned} \tag{18}$$

It can be deduced from Eq. (18) that $\sigma_{\delta b24z}$ is equal to $\sigma_{\delta b13z}$. This means that both δb_{24z} and δb_{13z} share the same standard deviation. Since all the structural errors are zero-symmetric, the means of expressions on both the left sides of Eq. (17) are eventually zero. Therefore, the non-synchronous error $\delta b_{\text{non-syn}}$ for the L/R mechanism can be represented by either δb_{24z} or δb_{13z}, whose standard deviation can be written as.

$$\sigma^2_{\delta b_{\text{non-syn}}} = 4h^2\sigma^2_{\Delta\alpha} + 4h^2\sigma^2_{\Delta\beta} + 2\sigma^2_{\Delta az} + 2\sigma^2_{\Delta l} \tag{19}$$

where $\sigma_{\delta b\text{non-syn}}$ denotes a standard deviation of the non-synchronous error of the L/R mechanism, whose mean ($\mu_{\delta b\text{non-syn}}$) is zero.

In terms of structural parameters and errors tabulated in Tables 4 and 5, the *1*st and *5*th levels are selected as analysis samples. The ranges of the non-synchronous error ($\delta b_{\text{non-syn}}$) and its standard deviation ($\sigma_{\delta b\text{non-syn}}$) are simulated as listed in Table 8.

Table 8

Non-synchronous error $\delta b_{\text{non-syn}}$ and its standard deviation $\sigma_{\delta b\text{non-syn}}$

Δa_{iz} /mm	$\Delta\alpha$ /°	$\Delta\beta$ /°	Δl /mm	$\delta b_{\text{non-syn}}$ /mm	$\sigma_{\delta b\text{non-syn}}$ /mm

Level 1	±0.05	±0.1	±0.1	±0.01	±0.744	0.248
Level 5	±0.25	±0.3	±0.3	±0.05	±2.250	0.750

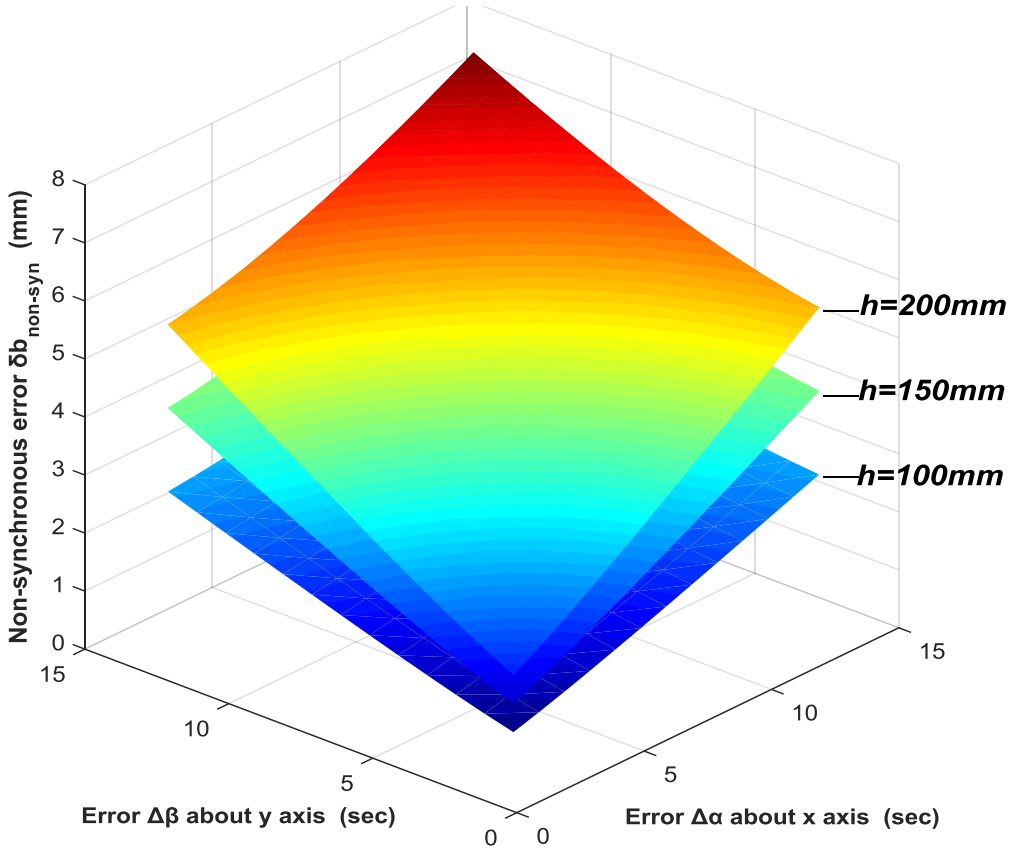

Fig. 8. Non-synchronous error $\delta b_{\text{non-syn}}$ varying with orientation errors $\Delta\alpha$, $\Delta\beta$ and semi-distance h of adjacent lead screws.

The relationship of $\delta b_{\text{non-syn}}$ and the orientation errors, $\delta\alpha$ and $\delta\beta$, and the semi-distance h of adjacent lead screws is illustrated in Fig. 8. We can observe that $\delta b_{\text{non-syn}}$ increases with the semi-distance of adjacent lead screws h. For a given h, $\delta b_{\text{non-syn}}$ keeps increasing continuously with the growth of the orientation errors, $\delta\alpha$ and $\delta\beta$, about the x-, y-axes, respectively. The location error, δa_{iz}, of a lead screw along the z-axis can be reduced through appropriate adjustment during assembly stage. The manufactured axial error (δl_s) of a lead screw makes an insignificant contribution to $\delta b_{\text{non-syn}}$. Therefore, in the assembly process, only orientation errors, $\delta\alpha$ and $\delta\beta$, should be closely controlled, the non-synchronous error $\delta b_{\text{non-syn}}$ can be guaranteed within the permitted tolerance criterion.

6. Conclusions

A comprehensive analysis on accuracy of each L/R mechanism is implemented, and some conclusions are drawn as follows:

(1) Both accuracy models (VAM and VDM) are proposed for output errors of the L/R mechanism. The axial error of a lead screw as one of component errors in the accuracy model, induced by transmission errors from the transmission chain, is analyzed through sensitivity analysis. Results from variance and range analysis indicate that manufactured precision of a lead screw is most significant.

(2) Correctness for the presented VDM is verified in detail, compared with VAM through DOE and MC simulation. End errors along *x*-, *y*-, and *z*- axes of a lead screw are investigated. The variation of them along with movement of a lead screw indicate that the axial error is kept constant and the error along *x*- axis is larger than that along *y*- axis within the movement range.

(3) The non-synchronous error of each L/R mechanism is deducted based on VDM, where a statistical model for the non-synchronous error is formulated. Factors such as orientation errors, $\delta\alpha$ and $\delta\beta$, of the backplane, are significant to the non-synchronous error of each L/R mechanism. They should be closely controlled during assembly process so that the tolerance criterion can be guaranteed.

The tolerance design for this L/R mechanism is attempted to carry out as the future work, and dynamic modeling and verification for performances will also be conducted subsequently.

Acknowledgements

This work is supported by the Research Fund of China Manned Space Engineering [grant number 050102]; the Key Research Program of the Chinese Academy of Sciences [grant number Y4A3210301]; the National Science Foundation of China [grant numbers 51775541, 51175494, 51575412, and 61128008], and the State Key Laboratory of Robotics Foundation.

References

[1] J.P. Zhou, Chinese space station project overall vision (in Chinese), Manned Spaceflight. 19 (2) (2013) 1-10.

[2] W.J. Xie, X.H. Luo, X.W. Zhang, et al., Microgravity Material Research in China:2016, Chin. J. Space Sci. 36 (5) (2016) 805-814.

[3] Y.R. Wang, G.L. Dai, J. Wang, et al., Microgravity Material Research in China:2012-2014, Chin. J. Space Sci., 34 (5) (2014) 757-764.

[4] Q.S. Liu, Y.X. Nie, M.F. Feng, et al., Progress on microgravity sciences in China, Chin. J. Space Sci. 26 (supp) (2006) 150-159.

[5] J.G. Liu, Y.M. Li, Y. Zhang, et al., Dynamic and control of a parallel mechanism for active vibration isolation in space station, Nonlinear Dynam. 76 (3) (2014) 1737-1751.

[6] J. P. Merlet, Parallel Robots, Springer-Verlay, Dordrecht, 2006.

[7] J.P. Merlet, Jacobian, manipulability, condition number, and accuracy of parallel robots, ASME J. Mech Des. 128 (1) (2006) 199-206.

[8] M. Weck, D. Staimer, Parallel Kinematic Machines Tools-Current State and Future Potentials, Ann. CIRP. 51 (2) (2002) 671-683.

[9] G.B. Hao, J.J. Yu, Design, Modelling and Analysis of a Completely-Decoupled XY Compliant Parallel Manipulator, Mech. Mach. Theory 102 (2016) 179-195.

[10] T. Huang, P.J. Bai, J.P. Mei, et al., Tolerance Design and Kinematic Calibration of a Four-Degrees-of-Freedom Pick-and-Place Parallel Robot, ASME J. Mech. Robot. 8 (6) (2016) 1-9.

[11] H.P. Jawale, H.T. Thorat, Comparison of Open Chain and Closed Chain Planar Two Degree of Freedom Manipulator for Positional Error, ASME J. Mech. Robot. 6 (2) (2014)1-7.

[12] G.E.E. Gojtan, G.P. Furtado, T.A. HessCoelho, Error Analysis of a 3-DOF Parallel Mechanism for Milling Applications, ASME J. Mech. Robot. 5 (3) (2013) 1-9.

[13] J.X. Fu, F. Gao, W.X. Chen, et al., Kinematic accuracy research of a novel six-degree-of-freedom parallel robot with three legs, Mech. Mach. Theory 102(2016) 86-102.
[14] X. Li, X.L. Ding, G.S. Chirikjian, Analysis of angular-error uncertainty in planar multiple-loop structures with joint clearances, Mech. Mach. Theory 91 (2015) 69-85.
[15] G.H. Cui, H. Zhang, D. Zhang, Analysis of the kinematic accuracy reliability of a 3-DOF parallel robot manipulator, Int. J. Adv. Robot. Syst. 12 (2015)1-11.
[16] S. Caro, P. Wenger, F. Bennis, et al., Sensitivity analysis of the orthoglide: A three-DOF translational parallel kinematic machine, ASME J. Mech. Des.128 (1) (2006) 392-402.
[17] F. Hao, J.P. Merlet, Multi-criteria optimal design of parallel manipulator based on interval analysis, Mech. Mach. Theory 40 (2) (2005) 157-171.
[18] J. Ryu, J. Cha, Volumetric error analysis and architecture optimization for accuracy of HexaSlide type parallel manipulators, Mech. Mach. Theory 38 (3) (2003) 227-240.
[19] J.W. Zhao, K.C. Fan, T.H. Chang, Error analysis of a serial-parallel type machine tool, J. Adv. Manuf. Technol. 19 (3) (2002) 174-179.
[20] K.C. Fan, H. Wang, J.W. Zhao, Sensitivity analysis of the 3-RPS parallel kinematic spindle platform of a serial-parallel machine tool l, J. Adv. Manuf. Technol. 43 (15) (2003) 1561-1569.
[21] F.C. Chen, H.H. Huang, Taguchi-Fuzzy based approach for sensitivity analysis of a four-bar function generator, Proc. Inst. Mech. Eng., Part C. 220 (9) (2006) 1413-1421.
[22] F.C. Chen, Y.F. Tzeng, W.R. Chen et al., The use of Taguchi method and principle component analysis for the sensitivity analysis of a dual-purpose six-bar mechanism, Proc. Inst. Mech. Eng., Part C. 223 (223) (2009) 733-741.
[23] J.G. Li, J. Ding, Y.X. Yao, et al., A new accuracy design for a 6-dof docking mechanism, Proc. Inst. Mech. Eng., Part C. 229 (18) (2015) 3473-3483.
[24] J.G. Li, J. Ding, Y.X. Yao, et al., Research on distribution pattern for central pose errors of 6-degree of freedom docking mechanism, Proc. Inst. Mech. Eng., Part C.231 (12) (2016) 2200-2210.
[25] A. Jeang, Combined parameter and tolerance design optimization with quality and cost, Int. J. Prod. Res. 39 (5) (2001) 923-952.
[26] A. Jeang, C.L. Chang, Concurrent optimization of parameter and tolerance design via computer simulation and statistical optimization, J. Adv. Manuf. Technol. 19 (6) (2002) 432-441.
[27] B.K. Rout, R.K. Mittal, Optimal manipulator tolerance design using hybrid evolutionary optimization technique, Int. J. Robot Autom. 22 (4) (2007) 263-271.
[28] B.K. Rout, R.K. Mittal, Tolerance design of robot parameters using Taguchi method, Mech. Syst. Signal. Pr. 120 (8) (2006) 1832-1852.
[29] B.K. Rout, R.K. Mittal, Parametric design optimization of 2-DOF R-R planar manipulator: A design of experiment approach, Robot. Cim-Int. Manuf. 24 (2) (2008) 239-248.
[30] W.Z. Huang, Y.M. Zhang, Tolerance analysis for design of multistage manufacturing process using number-theoretical net method, Int. J. Flex Manuf. Syst.16(2004) 65-90.
[31] T. Huang, D.J. Whitehouse, D.G. Chetwynd, A Unified Error Model for Tolerance Design, Assembly and Error Compensation of 3-DOF Parallel Kinematic Machines With Parallelogram Struts, Ann. CIRP. 51 (1) (2002) 297-301.
[32] P. Vischer, R. Clavel, Kinematic Calibration of the Parallel Delta Robot, Robotica. 16 (2)

(1998) 207-218.
[33] S. Briot, I.A. Bonev, Accuracy Analysis of 3T1R Fully-Parallel Robots, Mech. Mach. Theory 45 (5) (2010) 695-706.
[34] P.J. Bai, J.P. Mei, T. Huang, et al., Kinematic Calibration of Delta Robot Using Distance Measurements, Proc. Inst. Mech. Eng., Part C. 230 (3) (2016) 414-424.
[35] B.C. Wen, Machine Design Handbook (in Chinese), China Machine Press, Beijing, 2010.
[36] J.L. Devore, Probability and statistics for engineering and the sciences, Cengage Learning, Belmont, 2007.

Nomenclature

$\boldsymbol{a}_i$	nominal position of the ith lead screw in the frame $\{O_{A'}\}$
$\boldsymbol{b}_i$	nominal vector of an ideal contact between the ith slot on SSMP and the end of the ith lead screw in base frame $\{O_B\}$
$\boldsymbol{c}_i$	an vector of $\mathbf{R}(\boldsymbol{a}_i+l_i\boldsymbol{u}_i)$
DOE	design of experiment
e_i	differences of the standard deviation (σ_x, σ_y, or σ_z) of output errors from VAM and VDM (i=x, y, z)
$\mathbf{E}$	a 3×3 unit matrix
E(.)	average operator for in statistics
E_{s1}, E_{s2}	tolerance of tooth thickness of engaged gears 1 and 2, respectively
f_a	a central distance offset of engaged gears
f_i'	single tooth tangential composite deviation
F_i'	gear tangential total composite deviation
F_p	total cumulative pitch deviation
j	circumferential backlash
j_1	circumferential backlash induced by pith deviation of engaged gears
j_2	circumferential backlash induced by gear central distance offset
j_3	circumferential backlash induced by radical clearance of bearing
K	gear single transmission error
$\boldsymbol{l}_i$	nominal axial vector of ith lead screw
L/R	lock-or-release
MC	Monte Carlo
$\{O_{A'}\}$	frame attached on surface of backplane
$\{O_B\}$	frame attached on side surface of SSMP
$\boldsymbol{p}$	nominal displacement of frame $\{O_{A'}\}$ with respect to base frame $\{O_B\}$
$\mathbf{R_1}$	rotational matrix of frame $\{O_{A'}\}$ with respect to base frame $\{O_B\}$
$\mathbf{R_2}$	a hybrid rotary matrix for the ith lead screw
s	refers to a pitch of a lead screw
SSMP	Space Station Microgravity Platform
u_1, u_2	radical clearance of bearings match with gears 1 and 2
$\boldsymbol{u}_i$	unit vector $(u_x, u_y, u_z)^T$ of the ith lead screw
VAM	vector analysis model
VDM	vector differential model
α_v	normal pressure angle of engaged tooth

$\delta \boldsymbol{b}_i$	end error of the ith lead screw in frame $\{O_B\}$
$\delta \mathbf{R}$	perturbation of rotational matrix $\mathbf{R}$ for frame $\{O_{A'}\}$ to base frame $\{O_B\}$
$\delta \boldsymbol{u}_i$	deviation of $\boldsymbol{u}_i$
$\Delta \boldsymbol{a}_i$	position error $(\Delta a_x, \Delta a_y, \Delta a_z)$ of the ith lead screw fixed on the backplane
Δ_{ci}	antisymmetric tensor of vector $\boldsymbol{c}_i$
Δl	axial error of a lead screw induced by total transmission error of transmission chain
Δl_s	manufactured precision level of a lead screw
$\Delta \boldsymbol{p}$	displacement error $(\Delta x_p, \Delta y_p, \Delta z_p)^T$ of backplane
$\Delta \boldsymbol{\Omega}$	angular error $(\Delta\alpha, \Delta\beta, \Delta\gamma)^T$ of backplane about x-, y- and z- axis of base frame $\{O_B\}$
$\Delta_{\mathbf{R}}$	antisymmetric tensor of $\delta \boldsymbol{R}$
$\mu.$	mean of a statistic
$\sigma(.)$	the standard deviation operators in statistics